Electronic Supplementary Material (ESI) for Sustainable Energy & Fuels.

Supporting information

for

Construction of FeS_2@MoS_2 heterostructures for Enhanced Hydrogen Evolution

Dezhi Wang, [ab] Yuwen Song, [a] Ting Guo, [a] Ruoqi Liu, [a] Zhuangzhi Wu [a*b]

[a] *School of Materials Science and Engineering, Central South University, Changsha 410083, China*

[b] *Key Laboratory of Ministry of Education for Non-ferrous Materials Science and Engineering, Changsha 410083, China*

[*] Correspondence: Z Wu, Fax: +86-731-88830202; E-mail address: zwu@csu.edu.cn

Experiment

Synthesis of MoS_2

0.48 g of $Na_2MoO_4 \cdot 2H_2O$ and 265 μL HNO_3 were dissolved in 40 mL deionized water and the pH value was adjusted to 1. After magnetic stirring for 1 h, the mixture was transferred into 100 mL Teflon-lined stainless-steel autoclave, and then heated at 180 ℃ for 10 h to prepare MoO_3. Next, 0.3 g of CH_3CSNH_2 was dissolved in 25 mL deionized water, and mixed with 0.086 g of as-gained MoO_3. After stirring for 10 min, the mixture was put into 100 mL Teflon-lined autoclave and kept at 220 ℃ for 24 h. The precipitation was washed respectively using water and ethanol for thrice, collected by centrifugation, and then dried in the vacuum at 80 ℃ for 12 h.

Synthesis of FeS_2

0.16 g of NaOH and 0.54 g of $Fe(NO_3)_3 \cdot 9H_2O$ were dissolved in 40 mL deionized water and the pH value was adjusted to 1. After stirring for 1 h, the mixture was put into a 100 mL Teflon-lined stainless-steel autoclave, and kept at 180 ℃ for 10 h. After being naturally cooled, Fe_2O_3 could be collected. Subsequently, 0.3 g of CH_3CSNH_2 was dissolved in 25 mL deionized water, and mixed with 0.032 g of as-prepared Fe_2O_3. After stirring for 10 min, the mixture was put into 100 mL Teflon-lined autoclave and heated in an electric oven at 220 ℃ for 24 h. After being naturally cooled to room temperature, the black precipitation could be collected via centrifugation. And the product was washed respectively using deionized water and absolute ethyl alcohol for thrice and then dried at 80 ℃ for 12 h in the vacuum.

Materials characterization

The X-ray diffraction (XRD) patterns of samples were obtained by the D/max-2500 system, using Cu Kα radiation from 10° to 80°. Raman data were collected on an instrument LabRAMHR-800 from HORIBA. The surface compositions and chemical states were analyzed via X-ray photoelectron spectroscopy (XPS, Thermo Fischer, America) with an Al Kα source. And the morphology and microstructure of specimens were characterized by scanning electron microscopy (SEM, TESCAAN MIRA4) and transmission electron microscopy (TEM, Titan G260-300). Meanwhile, energy dispersive X-ray spectroscopy (EDX) attached to the SEM was used to examine the composition and distribution of elements.

Electrochemical measurements

Typically, 3 mg of the catalyst was mixed with 200 μL of anhydrous ethanol, 800 μL of ultra-pure water, and 80 μL of Nafion solution (5 wt %). After being sonicated for 30 min, 5 μL of the slurry was dropped onto the glassy carbon electrode in a diameter of 3 mm and dried naturally at room temperature. In this work, the HER data of all electrocatalysts were collected on the CHI660D electrochemical workstation (CH Instruments, China). Moreover, the reference electrode was saturated calomel, the counter electrode was carbon rod, and the electrolytes was 0.5 M H_2SO_4. The polarization curves were obtained by linear sweep voltammetry (LSV) with a scanning speed of 2 mV s^{-1}. Besides, the Tafel curves were carried out on the polarization as follows,

$$\eta = b\log|j| + a \quad (1)$$

where η is the overpotential, b is the Tafel slope, j is the current density, and a is the initial potential of all the samples.

The electrochemical impedance spectroscopy was obtained at an overpotential of 200 mV with the frequencies ranging from 100 kHz to 1 Hz. In order to analyze the electrochemically active surface area (ECSA), we established the linear relationship between the current density and the scanning rate by cyclic voltammetry (CV) with various scan rates (20, 40, 60, 80, 100, 120 and 140 mV s^{-1}).[1] The fitted slope was the electrochemical double-layer capacitance (C_{dl}), and the ECSA could be calculated as follows,

$$A_{ECSA} = \frac{C_{dl}}{C_0} \quad (2)$$

where C_0 is the generally specific capacitance, which could be regarded as a constant.

To explore the electrochemical stability, the catalyst was coated on carbon cloth and tested by continuous CV and chronoamperometry. And the long-term cycling test was carried out by repeating up to 2000 CV cycles at the potential between -0.4 and 0.1 V vs RHE with 50 mV s^{-1}. The chronoamperometric analysis is a constant current test for 10 h when the electrocatalyst reaches a fixed potential for 10 mA cm^{-2} to investigate the attenuation of current density.

Computational methods

Typically, the density functional theory (DFT) calculations were carried out by the Vienna ab initio simulation package code, where the electron-ion interactions

were described via the projected augmented-wave potentials.[2, 3] The exchange-correlation interactions were treated by the Perdew-Burke-Enzerhof pseudopotentials of generalized gradient approximation.[4] The plane-wave energy cutoff was set as 500 eV, and the convergence threshold was set as 0.05 eV per angstrom in force. For all calculations, the Brillouin zone was simulated by gamma centered Monkhorst-Pack scheme, in which the 2 x 2 x 1 grid was adopted for sampling.[5]

The Gibbs free energy of hydrogen adsorption (ΔG_{H*}) was calculated as follows:

$$\Delta G_{H*} = \Delta E_{pot} + \Delta E_{ZPE} - T\Delta S \quad (3)$$

where the ΔE_{pot}, ΔE_{ZPE} and the ΔS were referred as the changes of potential energy, zero-point energy and entropy. The zero-point energy was calculated by the summation of all vibrational frequencies as follows:

$$E_{ZPE} = \frac{1}{2}\sum \hbar\nu \quad (4)$$

where the ν corresponded to the vibriational frequency of each normal mode.[6]

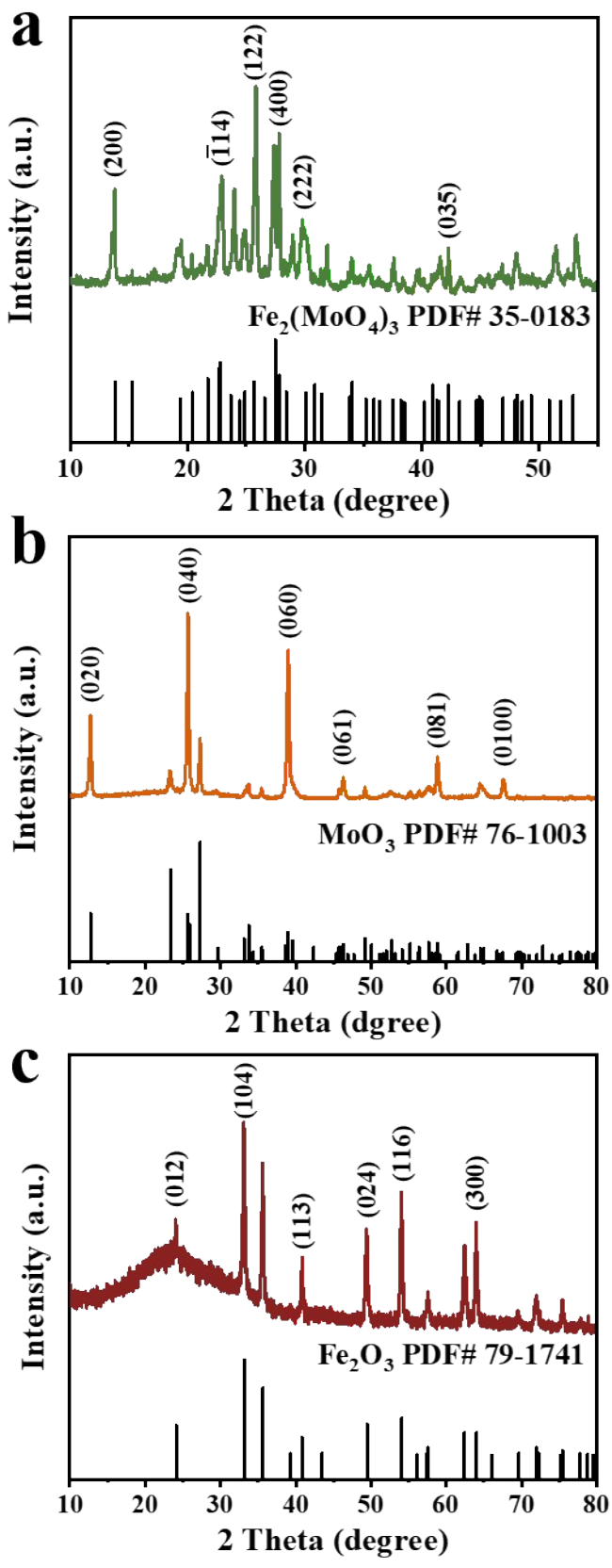
a
Intensity (a.u.)
(200)
(-114)
(122)
(400)
(222)
(035)
Fe2(MoO4)3 PDF# 35-0183
10
20
30
40
50
2 Theta (degree)
b
Intensity (a.u.)
(020)
(040)
(060)
(061)
(081)
(0100)
MoO3 PDF# 76-1003
10
20
30
40
50
60
70
80
2 Theta (dgree)
c
Intensity (a.u.)
(012)
(104)
(113)
(024)
(116)
(300)
Fe2O3 PDF# 79-1741
10
20
30
40
50
60
70
80
2 Theta (degree)

Fig. S1 XRD patterns of (a) $Fe_2(MoO_4)_3$, (b) MoO_3 and (c) Fe_2O_3.

Table S1. Mo 3d and S 2p XPS results of various samples.

Compound	Line	Peak B.E. (eV)	Area C.P.S. (eV)	Ref.
FeS_2@MoS_2	Mo $3d_{5/2}$ (1T)	228.3	48708.7	7
	Mo $3d_{3/2}$ (1T)	231.5	32550.6	
	Mo $3d_{5/2}$ (2H)	229.3	24057.4	
	Mo $3d_{3/2}$ (2H)	232.5	16015.3	
	S $2p_{3/2}$ (Mo-S 1T)	161.2	29263.2	8
	S $2p_{1/2}$ (Mo-S 1T)	162.5	20004.1	
	S $2p_{3/2}$ (Mo-S 2H)	162.3	4741.0	
	S $2p_{1/2}$ (Mo-S 2H)	163.9	3115.5	
	S $2p_{3/2}$ (Fe-S)	163.3	7814.9	9
	S $2p_{1/2}$ (Fe-S)	164.3	5209.9	
MoS_2	Mo $3d_{5/2}$ (1T)	228.7	63019.4	10
	Mo $3d_{3/2}$ (1T)	231.9	42110.8	
	Mo $3d_{5/2}$ (2H)	229.7	29050.9	
	Mo $3d_{3/2}$ (2H)	232.9	19431.0	
	S $2p_{3/2}$ (Mo-S 1T)	161.6	29757.1	
	S $2p_{1/2}$ (Mo-S 1T)	162.9	20218.7	
	S $2p_{3/2}$ (Mo-S 2H)	162.8	9628.1	
	S $2p_{1/2}$ (Mo-S 2H)	163.9	6564.5	
FeS_2	S $2p_{3/2}$ (Fe-S)	162.6	34719.0	11

S $2p_{1/2}$ (Fe-S)	163.8	20725.1

Table S2. Comparison of the electrocatalytic activity over FeS_2@MoS_2 with other related electrocatalysts for HER in 0.5 M H_2SO_4.

Catalysts	Electrode/supporting material	Loading (mg cm^{-2})	Onset (mV)	η_{10} (mV)	Tafel slope (mV dec^{-1})	Ref.
C-1T MoS_2	GC	0.280	-113	-156	42.7	12
2D MoS_2 nanosheets	GC	1.019×10^{-3}	~-480	—	40	13
	EPPG	1.267×10^{-3}	~-450	—	74	
	BDD	1.267×10^{-3}	~-450	—	90.9	
	SPE	1.267×10^{-3}	~-440	—	92	
$Co_{0.85}Se$ NWs	GC	0.283	-165	—	58	14
$Co_{0.85}Se$@CNWs	GC	0.283	-138	-214	43.4	
rGO/MoS_2-S	GC	2.000	-160	-250	72	15
MoS_2/RGO	GC	0.285	-100	-156	41	16
MoS_2/CNTs	GC	0.136	-90	-184	44.6	17
MoS_2@SWNT film	GC	—	-92	-152	41	18

AS-rich MoS_2 nanosheet	GC	0.285	-180	-220	68	19
Defect rich MoS_2 nanosheets	GC	0.285	-120	—	50	20
H-MoS_2	GC	1.000	-50	-167	70	21
Bulk MoS_2	GC	0.213	—	—	164	22
hH-MoS_2	GC	0.205	-112	-214	74	23
MoS_2/CNFs	GC	0.212	-224	-342	110	24
Co_9S_8@MoS_2/CNFs	GC	0.212	-64	-190	110	
CoS_2@MoS_2	GC	0.213	-190	-276	60	25
MoS_2/CuS	GC	0.471	-150	-290	63	26
MoS_2/WS_2/rGO	GC	1.230	-113	-157	44	27
g-C_3N_4/30% FeS_2/MoS_2	GC	0.710	-107	-193	87.7	28
Fe-MoS_2NF	CC	8.900	-100	-136	82	29
MoS_2/FeS_2	CC	1.000	—	-134	78.6	30
FeS_2@MoS_2	GC	0.213	-133	-231	58	This work

Key: —: Value unknown; GC: glassy carbon; EPPG: edge plane pyrolytic graphite; BDD: boron doped diamond; SPE: screen-printed graphite electrode; CC: carbon cloth.

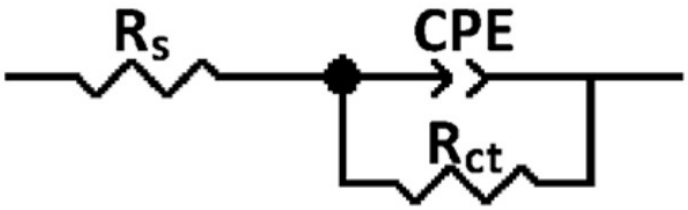

Fig. S2 Equivalent circuit model for electrochemical impedance tests. R_S is the solution resistance. CPE is the constant phase element of the electric double layer, and R_{ct} in the low frequency region reflects the charge transfer resistance during HER.

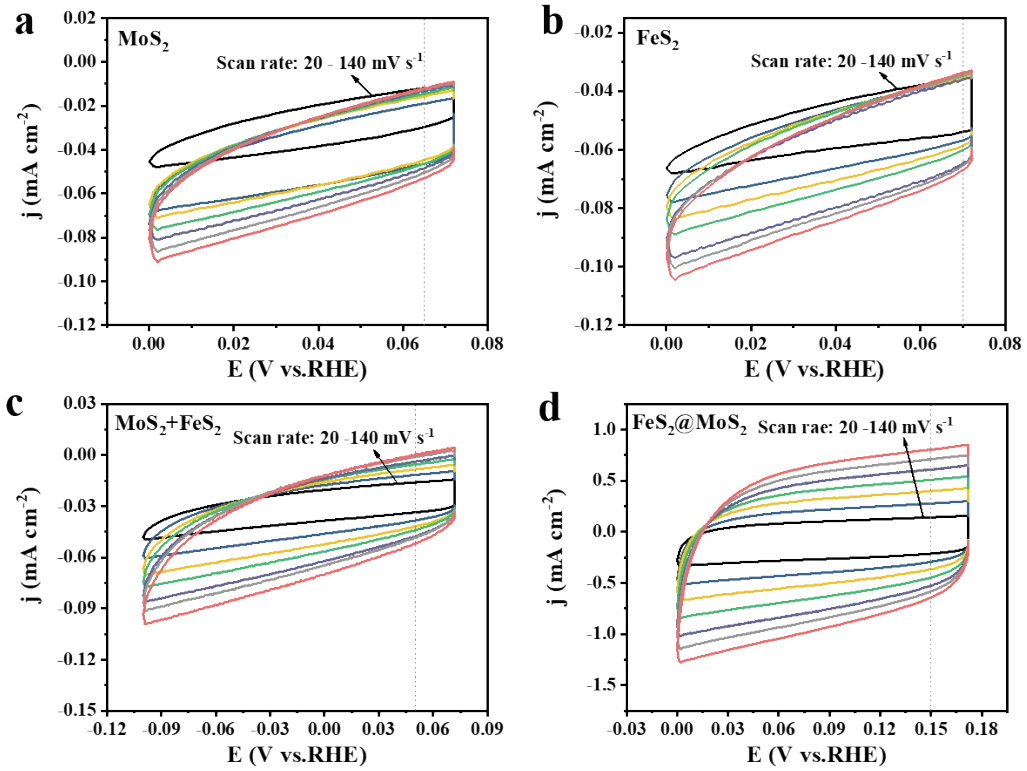

Fig. S3 CV curves at different scan rates of (a) MoS_2, (b) FeS_2,

(c) MoS_2+FeS_2, and (d) FeS_2@MoS_2.

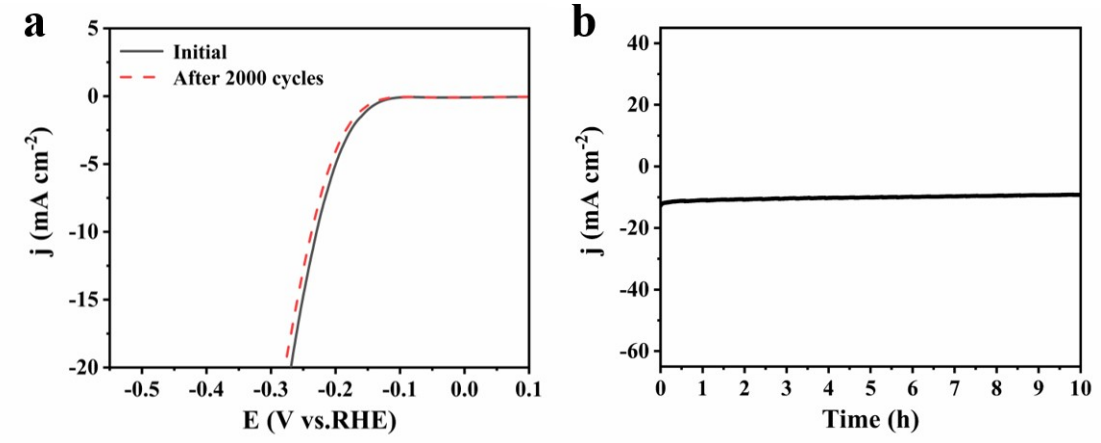

Fig. S4 (a) Polarization curves before and after 2000 cycles and (b) chronopotentiometry of the FeS_2@MoS_2 catalyst performed at 10 mA cm^{-2} for 10 h.

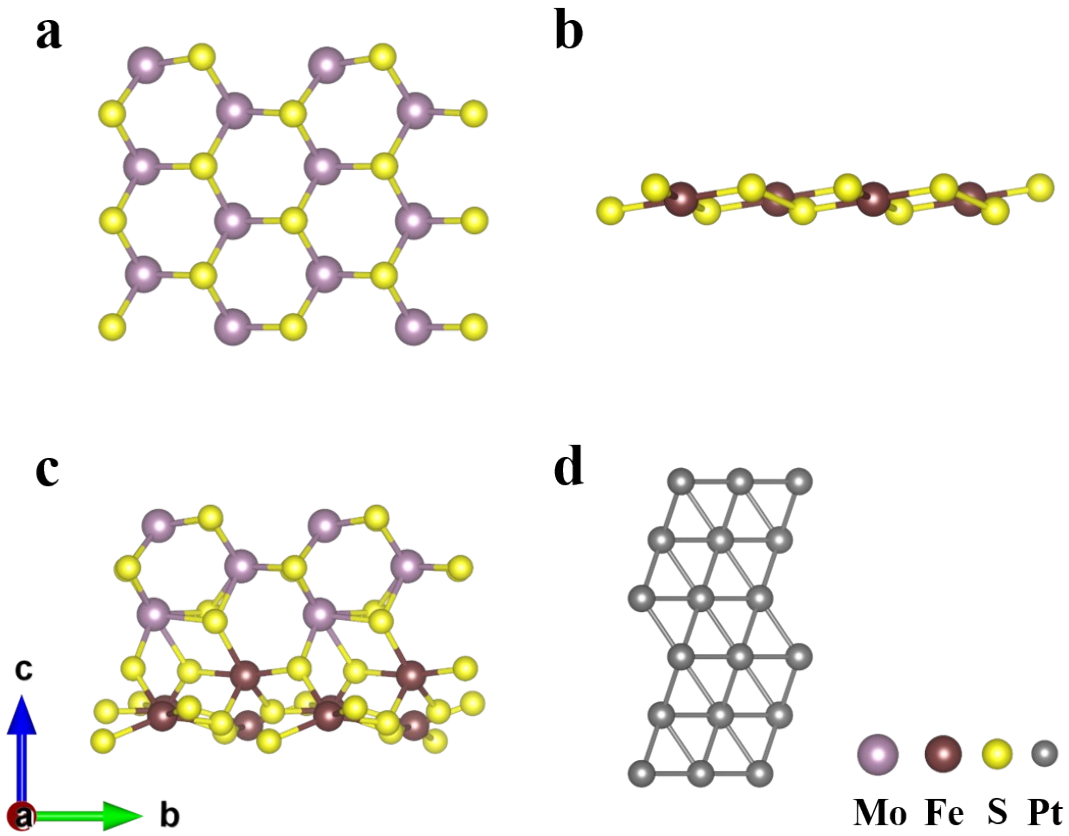

Fig. S5 The theoretical models of (a) MoS_2, (b) FeS_2, (c) FeS_2@MoS_2 and (d) Pt.

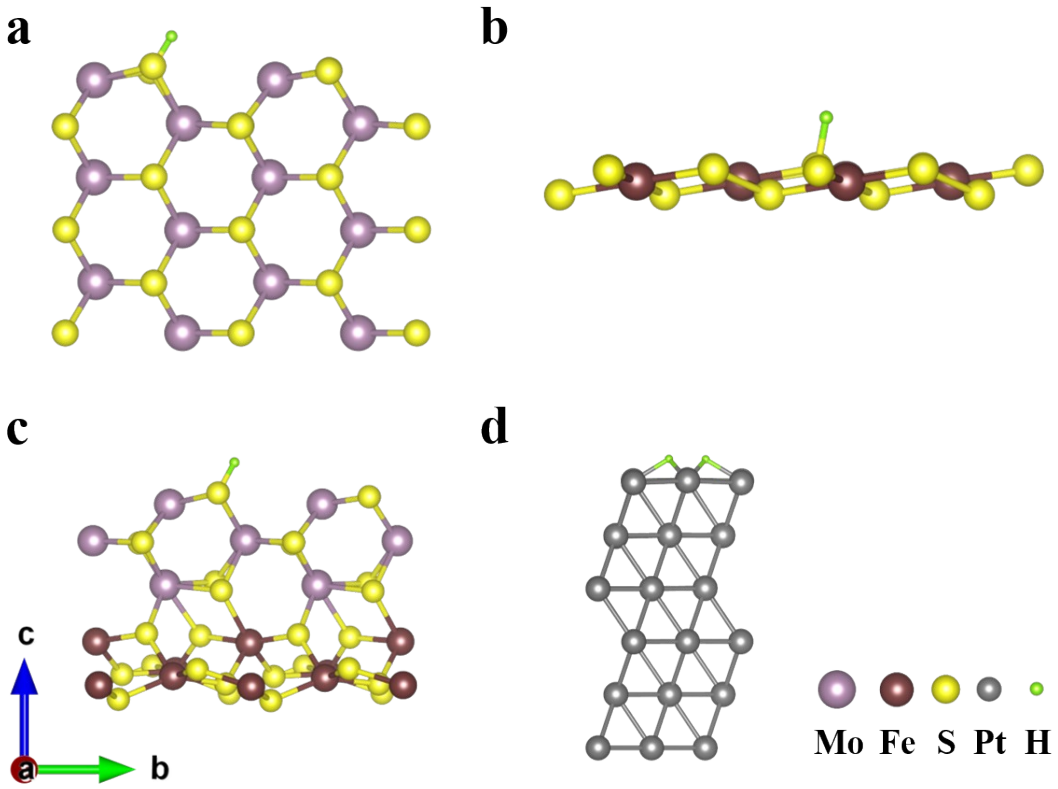

Fig. S6 The theoretical models of (a) H*MoS_2, (b) H*FeS_2, (c) H*FeS_2@MoS_2 and (d) H*Pt.

References:

1 S. Trasatti and O. A. Petrii, *J. Electroanal. Chem.*, 1992, **327**, 353-376..

2 G. G. Kresse and J. J. Furthmüller, *Phys. Rev. B Condens. Matter*, 1996, **54**, 11169-11186.

3 P. Chl, *Phys. Rev. B*, 1994, **50**, 17953-17979.

4 J. P. Perdew, K. Burke and M. Ernzerhof, *Phys. Rev. Lett.*, 1996, **77**, 3865-3868.

5 X. Zhang, X. Liu, G. Liang, L. Rui and Y. Bing, *J. Quant. Spectrosc. Radiat. Transfer*, 2016, **168**, 66-77.

6 Y. Li, S. H. Chan and Q. Sun, *Nanoscale*, 2015, **7**, 8663-8683.

7 K. Chang, X. Hai, H. Pang, H. Zhang, L. Shi, G. Liu, H. Liu, G. Zhao, M. Li and J.

Ye, *Adv. Mater.*, 2016, **28**, 10033-10041.

8 Q. Zhang, Y. Wang, X. Zhu, X. Liu and H. Li, *Appl. Surf. Sci.*, 2021, **556**, 149768.

9 B. Tang, Z. Yu, H. L. Seng, N. Zhang, X. Liu, Y. Zhang, W. Yang and H. Gong, *Nanoscale*, 2018, **10**, 20113-20119.

10 N. T. Xuyen and P. J. Ting, *Chem. Eur. J.*, 2017, **23**, 17348-17355.

11 J. Xia, J. Jiao, B. Dai, W. Qiu, S. He, W. Qiu, P. Shen and L. Chen, *RSC Adv.*, 2013, **3**, 6132-6141.

12 Y. Li, L. Wang, S. Zhang, X. Dong, Y. Song, T. Cai and Y. Liu, *Catal. Sci. Technol*., 2017, **7**, 718-724.

13 S. J. Rowley-Neale, D. A. Brownson, G. C. Smith, D. A. Sawtell, P. J. Kelly and C. E. Banks, *Nanoscale*, 2015, **7**, 18152-18168.

14 B. Sun, X. Wang, D. Yang and Y. Chen, *RSC Adv*, 2019, **9**, 17238-17245.

15 S. Kamila, B. Mohanty, A. K. Samantara, P. Guha, A. Ghosh, B. Jena, P. V. Satyam, B. K. Mishra and B. K. Jena, *Sci. Rep.*, 2017, **7**, 8378.

16 Y. Li, H. Wang, L. Xie, Y. Liang, G. Hong and H. Dai, *J. Am. Chem. Soc.*, 2011, **133**, 7296-7299.

17 Y. Yan, X. Ge, Z. Liu, J. Wang, J. Lee and X. Wang, *Nanoscale*, 2013, **5**, 7768.

18 D. Liu, W. Xu, Q. Liu, Q. He, Y. A. Haleem, C. Wang, T. Xiang, C. Zou, W. Chu, J. Zhong, Z. Niu and L. Song, *Nano Res*, 2016, **9**, 2079-2087.

19 N. Liu, Y. Guo, X. Yang, H. Lin, L. Yang, Z. Shi, Z. Zhong, S. Wang, Y. Tang and Q. Gao, *ACS Appl. Mater. Inter*., 2015, **7**, 23741-23749.

20 J. Xie, H. Zhang, S. Li, R. Wang, X. Sun, M. Zhou, J. Zhou, X. Lou and Y. Xie,

Adv. Mater., 2013, **25**, 5807-5813.

21 J. Zhang, S. Liu, H. Liang, R. Dong and X. Feng, *Adv. Mater.*, 2015, **27**, 7426-7431.

22 D. Wang, X. Zhang, S. Bao, Z. Zhang, H. Fei and Z. Wu, *J. Mater. Chem. A*, 2017, **5**, 2681-2688.

23 B. Guo, K. Yu, H. Li, H. Song, Y. Zhang, X. Lei, H. Fu, Y. Tan and Z. Zhu, *ACS Appl. Mater. Inter.*, 2016, **8**, 5517-5525.

24 H. Zhu, J. Zhang, R. Y. Zhang, M. Du, Q. Wang, G. Gao, J. Wu, G. Wu, M. Zhang, B. Liu, J. Yao and X. Zhang, *Adv. Mater.*, 2015, **27**, 4752-4759.

25 Q. Wei, Z. Ye, X. Ren, X. Li and F. Fu, *J. Alloys Compd.*, 2020, **835**, 155264.

26 L. Zhang, Y. Guo, A. Iqbal, B. Li, D. Gong, W. Liu, K. Iqbal, W. Liu and W. Qin, *Int. J. Hydrogen Energ.*, 2018, **43**, 1251-1260.

27 H. J. Lee, S. W. Lee, H. Hwang, S. I. Yoon, Z. Lee and H. S. Shin, *Mater. Chem. Front.*, 2021, **5**, 3396-3403.

28 Y. Li, S. Zhu, Y. Xu, R. Ge, J. Qu, M. Zhu, Y. Liu, J. M. Cairney, R. Zheng, S. Li, J. Zhang and W. Li, *Chem. Eng. J.*, 2021, **421**, 127804.

29 Z. Xue, M. Xiao, Q. Lu, Q. Li and X. Yang, *Electrochim. Acta*, 2017, **249**, 72-78.

30 Y. Chen, Z. Peng, Y. Guo, S. Guan and X. Fu, *Solid State Sci.*, 2020, **101**, 106156.